Supporting Information for:

Novel Preparation Methods of ^{52}Mn for ImmunoPET Imaging

Stephen A. Graves, Reinier Hernandez, Jesper Fonslet, Christopher G. England, Hector F. Valdovinos, Paul A. Ellison, Todd E. Barnhart, Dennis R. Elema, Charles P. Theuer, Weibo Cai, Robert J. Nickles and Gregory W. Severin.

Contents:

I. Rudimentary dosimetry comparison between ^{52}Mn and ^{89}Zr, and the influence of ^{54}Mn:

In order to assess the acceptability of ^{52}Mn as an immunoPET label, it is useful to make a dosimetric comparison to ^{89}Zr. Due to the high energy gammas from both isotopes, a good first order evaluation is to evaluate the dose to the whole body, liver, and bone marrow due to accumulations in two common accumulating structures, namely the liver and bone. Clearly before translation more data and detailed dosimetry is required, however this analysis aims at providing a reasonable estimate.

The biological half-life of Zr and Mn in mice tibia are 97 days and 263 days respectively[1, 2], therefore the residence time in the bone is assumed to be entirely determined by the physical decay. For the liver, the clearance half-life observed in mice for TRC105 is approximately 50 h for ^{89}Zr-DFO-TRC105 and 173 h for ^{52}Mn-DOTA-TRC105. Using these numbers without allometric scaling however makes a distorted picture for the human dosimetry. One possibility to estimate residence times in humans is to assume that any activity in the bones is transchelated from the initial tracer, and any activity in the liver will eventually be metabolized into a bio-available state. Therefore the clearance half-lives of the free elements for the bones, 21years[3] for Zr and 8.5 years[2] (scaled) for Mn, can be used to determine the residence time in the bone, and the slow-phase biological half-life for the free elements, 7 days[4] for Zr and 39 days[5] for Mn, can be used to calculate the liver residence times. By these approximations, OLINDA is used to calculate effective dose per MBq in each organ with the results shown in table S1 (note: uptake phase is ignored as it is short compared to the clearance time).

Table S1: Effective dose in mSv to liver, bone marrow, or whole body per MBq accumulated activity in either the liver or bone as the source organ (after uptake phase). Calculations were performed with OLINDA[6], using the 75 kg adult male phantom. The effective half-life of the nuclides in the liver was calculated using the slow phase of the biological half-life of the free metals, 7 days for Zr, and 39 days for Mn. As bone desorption rates for these elements are very slow (8.5 years for Mn and 21 years for Zr) the effective half-life for each nuclide in the bone is simply the physical half-life.

	Eff. half-life (d)		Dose to Liver (mSv/MBq)		Dose to Red Marrow (mSv/MBq)		Whole Body (mSv/MBq)	
	^{52}Mn	^{89}Zr	^{52}Mn	^{89}Zr	^{52}Mn	^{89}Zr	^{52}Mn	^{89}Zr
1MBq Liver	4.9	2.2	30.6	6.5	1.4	0.2	2.7	0.5
1MBq Bone	5.6	3.3	0.9	0.2	5.5	2.3	1.6	0.5

In general, the results in table S1 demonstrate that the patient dose is approximately 5 times higher when using ^{52}Mn compared to equal activity accumulation of ^{89}Zr. In practice this will be mitigated to a small degree by the slightly higher abundance of positron emission from ^{52}Mn (29.6% for ^{52}Mn vs. 22.7% for ^{89}Zr) meaning that less injected activity is needed for the same detector response. Additionally, if injected activities are scaled for a desired response at a late time-point, equivalent imaging will require less injected activity of ^{52}Mn compared to ^{89}Zr due to the half-life difference. As an example, to get the same positron rate at 10 days post-injection, three times more ^{89}Zr would need to be injected than ^{52}Mn. Therefore if imaging is intended to be done at late time points, and the injected activity is scaled accordingly, the dosimetry difference is not quite as pronounced.

Turning to the influence of ^{54}Mn on the dosimetry, on average ^{54}Mn comprised 0.4% of the overall activity at EOB. As a reasonable estimation we assume that at injection this has grown to 0.5%, meaning that for every 1MBq of ^{52}Mn injected there is also 5 kBq of ^{54}Mn injected in the same chemical form. Using the biological half-lives as above, it is possible to calculate the influence of ^{54}Mn upon the dosimetry, as presented in Table S2.

Table S2: Effective dose to target organs from 5 kBq ^{54}Mn accumulated in either the liver or bone (corresponding to 1MBq of ^{52}Mn accumulated).

	Eff. half-life (d)	Dose to Liver (mSv/5 kBq)	Dose to Red Marrow (mSv/5 kBq)	Whole Body (mSv/5 kBq)
5 kBq Liver	35	0.25	0.01	0.02
5 kBq Bone	283	0.06	0.07	0.09

From table S2 it is clear that a safe estimate considering the presence of ^{54}Mn is that it will not alter the personal dosimetry of a patient by more than about 5%, making it a minor contribution. However there are other quality-of-life considerations with injections of long-lived radioactivity (e.g. trouble at security screenings in airports, or cultural stigma) which might prompt the use of enriched ^{52}Cr as a target material to limit ^{54}Mn. As with any patient care, there is a delicate balance between cost, benefit, and quality of life that must be met on an individual basis. However, the *dose* from ^{54}Mn should not weigh heavily, especially if the dose from ^{52}Mn is deemed acceptable.

II. Biodistribution Data:

The full ex vivo biodistribution is presented numerically in table S3.

Table S3: *Ex vivo* Free ^{52}Mn and ^{52}Mn-DOTA-TRC105 biodistribution data obtained following the last PET time point. Animals were sacrificed, and tissue samples were isolated, washed with saline, dried, weighed, and gamma counted.

Tissue	Free ^{52}Mn (%ID/g) (n = 4)	^{52}Mn-DOTA-TRC105 (%ID/g) (n = 3)
4T1 Tumor	2.9 ± 0.2	12.8 ± 2.5
Blood	0.27 ± 0.14	11.5 ± 2.5
Skin	1.6 ± 0.2	2.7 ± 1.0
Muscle	1.9 ± 0.3	1.2 ± 0.2
Bone	2.3 ± 0.6	11.9 ± 5.1

Heart	7.0 ± 0.3	3.3 ± 0.4
Lung	3.8 ± 0.5	6.0 ± 0.7
Liver	9.9 ± 0.6	7.8 ± 0.6
Kidney	19.2 ± 1.1	5.9 ± 0.6
Spleen	2.2 ± 0.6	12.3 ± 1.0
Pancreas	29.4 ± 6.0	2.6 ± 0.3
Stomach	8.1 ± 2.0	1.9 ± 0.8
Intestine	1.7 ± 0.3	3.5 ± 1.3
Tail	0.8 ± 0.2	2.8 ± 0.7
Brain	2.30 ± 0.07	0.46 ± 0.06
Thyroid	15.1 ± 2.0	-

III. Imaging characteristics of ^{52}Mn:

As a semi-quantitative comparison of resolution, Derenzo phantom images are presented in figure S1 for ^{52}Mn, ^{64}Cu, ^{76}Br and ^{124}I.

Figure S1: Derenzo resolution phantom comparison of ^{52}Mn, ^{64}Cu, ^{76}Br, and ^{124}I on a Siemens Inveon MicroPET/CT scanner. From large to small, the hole separations are 5 mm, 4mm, 3 mm, 2.5 mm, and 2 mm.

^{52}Mn ^{64}Cu ^{76}Br ^{124}I
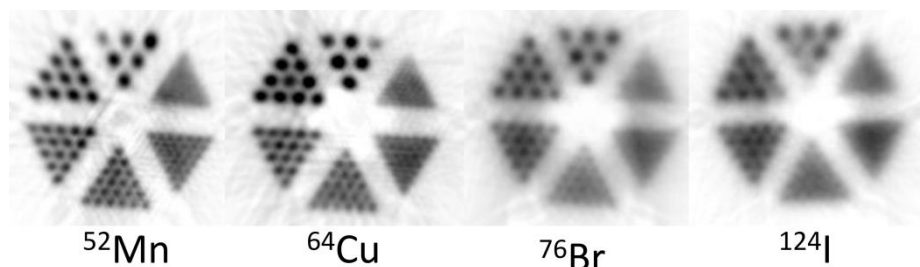
References

1. Ishinishi, N., and Morishige, T. (1969) A Study on the Distribution of ^{95}Zr-^{95}Nb Administered Subcutaneously to Rats: Comparison between Young and Adult Rats, *Journal of Radiation Research 10*, 101-106.
2. O'Neal, S. L., Hong, L., Fu, S., Jiang, W., Jones, A., Nie, L. H., and Zheng, W. (2014) Manganese accumulation in bone following chronic exposure in rats: Steady-state concentration and half-life in bone, *Toxicology letters 229*, 93-100.
3. Greiter, M. B., Giussani, A., Höllriegl, V., Li, W. B., and Oeh, U. (2011) Human biokinetic data and a new compartmental model of zirconium—A tracer study with enriched stable isotopes, *Science of the Total Environment 409*, 3701-3710.
4. Mealey, J. (1957) Turn-over of carrier-free zirconium-89 in man. *Nature*, 179, 673-674
5. Mahoney, J. P., and Small, W. J. (1968) Studies on manganese: III. The biological half-life of radiomanganese in man and factors which affect this half-life, *Journal of Clinical Investigation 47*, 643.
6. Stabin, M. G., Sparks, R. B., and Crowe, E. (2005) OLINDA/EXM: the second-generation personal computer software for internal dose assessment in nuclear medicine, *Journal of Nuclear Medicine 46*, 1023-1027.